中の塩素原子濃度が相対的に低下し，塩素の連続付加反応が DCAA で停止したため，TCAA 生成比率が低下したことが原因と思われる．

3）酸共存下におけるハロ酢酸類の生成

次亜塩素酸ナトリウムに食品添加物として使用が認められている各種酸を混和し，生成する消毒副生成物の量を調べた．次亜塩素酸ナトリウムに酒石酸，コハク酸，フマル酸，塩酸を加え混和した溶液では，消毒副生成物生成量に大きな変化は見られなかったが，クエン酸を添加した場合，経時的な DCAA 及び TCAA 濃度が増加した．Streicher らは，クエン酸が次亜塩素酸と反応することにより，クロロホルムやハロアセトンと共に DCAA や TCAA が生成することを明らかとしている[27]．その反応メカニズムとしては，クエン酸が次亜塩素酸により酸化されアセトンジカルボン酸となり，さらに，酸性条件下にエノール化され，求電子付加反応に基づき 2 位及び 4 位の炭素が連続的に塩素化されハロアセトンが生成し，さらに分解反応が進行し，クロロホルムと共に DCAA 及び TCAA が生成すると考えられる (Fig.10)．また，次亜塩素酸・リンゴ酸混液での反応では初期段階において DCAA の生成が確認されたが，次亜塩素酸・クエン酸混液に比べ，低い生成量に止まった．昨年度の研究において報告したように，リンゴ酸は次亜塩素酸による酸化反応後，連続的な塩素付加反応が進行するが，主反応生成物は抱水クロラールとなり，一般的に用いられる弱酸性溶液での塩素殺菌処理の場合には，カルボン酸の脱炭酸反応が先行するため，ハロ酢酸への分解経路はほとんど進行しないと考えられる．

4）水洗浄による消毒副生成物の除去効果の検討

カットキャベツの塩素殺菌工程で生成した DCAA や TCAA は，水洗浄を行うことにより減少させることが可能であった．また，水洗浄処理後のカットキャベツ中 DCAA 量(0.0634 mg/kg)をもとに，野菜類からの DCAA 摂取量の推定を試みた．野菜類の摂取量は，独立行政法人国立健康・栄養研究所の平成 14 年度厚生労働省国民栄養調査結果[28]における食品群別摂取量（全国，年齢階級別）を参考として，20 歳以上の一人一日当たりの野菜類摂取量を 285.0 g とした．この結果，野菜類より摂取される DCAA 一日摂取量は 0.28 μg/kg/day となる．水道水では，De Angelo らの報告[29]に基づく DCAA の用量相関解析から 10^{-5} 発がんリスクに相当する VSD を 1.43 μg/kg/day と算定し，水質基準値を 0.04 mg/l に設定している．このため，VSD に対する野菜類からの DCAA 摂取量の寄与率は 19.4%である．また同様に，各年齢別の寄与率について算定すると 16.1 - 39.4%であり，各年齢別において寄与率に若干の違いがみられるが，寄与率が 40%を越える群はなかった．さらに，平成 10-11 年度における水道事業者の DCAA 検出状況は最大で 0.02 mg/l であるため，体重 50kg のヒトが一日 2L の水を飲むと仮定した場合，水道水からの一日摂取量は 0.8 μg/kg/day となる．このため，水道水と野菜類から算定される一日摂取量は最大値で 1.08 μg/kg/day であり，総摂取量においても VSD を下回る結果となった．

今回，野菜類全体としての摂取量の推定を行っているが，実際において次亜塩素酸により殺菌処理されるカット野菜の量は，

野菜類全体の一部分であり，さらに，一般に塩素殺菌後には流水により十分にすすぎ洗いが行われることから，DCAA 摂取量全体からみたカット野菜からの寄与率は，今回算定した数値より低くなることが予想される．

また，TCAA に関しては，De Angelo らの報告[30]を基に TDI を 32.5 μg/kg/day と算定しており，水質基準値を 0.2 mg/l に設定している．今回の実験より，カット野菜の塩素処理後の TCAA 生成量は DCAA に比べて低く，野菜類からの摂取量も低く見積もられるため，健康への影響はほとんどないと思われる．

E. 結論

今回，カット野菜を次亜塩素酸ナトリウムにより殺菌処理を行うことにより，ジクロロ酢酸及びトリクロロ酢酸が生成し，次亜塩素酸ナトリウムにクエン酸を混和して長時間放置した場合，トリクロロ酢酸の生成量が増加していくことが明らかとなった．しかし，カット野菜を次亜塩素酸ナトリウムにより殺菌処理後，水洗浄をおこなうことで，洗浄後にはハロ酢酸濃度が低下し，化学的リスクを低減化させることができた．

次亜塩素酸ナトリウムは，野菜や魚介類加工品など生鮮食品の微生物学的危害を防止する上で重要な役割を果たしており，近年問題となっているノロウィルスによる食中毒危害防止のためにも欠かせない添加物である．今後とも微生物学的リスクを十分に考慮した上で化学的リスク評価を行っていく必要があると考えられる．

F. 健康危険情報

なし

G. 参考論文

1) Rook, J.J.: Water Treatment and Examination, 21(3), p259 (1972)

2) Rook, J.J.: Water Treatment and Examination, 23(2), p234-243 (1974)

3) WHO: Guidelines for Drinking-water Quality 3rd Ed. (2004)

4) Susan D. Richardson: Trends in Analytical Chemistry, 22(10), p666-684 (2003)

5) Official Journal of the European Communities Counci Directive 98/83/EC (1998)

6) 厚生労働省令第百一号:水質基準に関する省令 (2003)

7) Hidaka, T. et al.: 食品衛生学雑誌, 32(4), p308-314 (1991)

8) Hidaka, T. et al.: 食品衛生学雑誌, 33(3), p267-273 (1992)

9) Hidaka, T. et al.: 食品衛生学雑誌, 35(4), p357-364 (1994)

10) Imaeda, K.. et al.: 衛生化学, 40(6), p527-533 (1994)

11) Tiefel, P., Guthy, K.: Milchwissenschaft, 52(12), p686-691 (1997)

12) Resch, P., Guthy, K.: Deutsche Lebensmittel-Rundschau, 95, p418-523 (1999)

13) Resch, P., Guthy, K.: Deutsche Lebensmittel-Rundschau, 96, p9-16 (2000)

14) Chang, T. L. et al.: Analytical Letters, 21(11), p2049-2067 (1988)

15) 官報 第3378号、厚生労働省令第七十五号、p1 (2002)
16) 厚生労働省医薬食品局食品安全部基準審査課長通知:食安基発第 0825001 号 (2004)
17) 厚生省:食品添加物公定書第7版, p269 (1999)
18) Urbansky E. T. : J. Envion. Monit., 2, p285-291 (2000)
19) Takino, M. : Analyst, 125, p1097-1102 (2000)
20) 楢崎久武：分析化学, 55, p23-27 (2006)
21) 長谷川美典: カット野菜ハンドブック, p170-173 (2002)
22) 厚生労働省医薬食品局食品安全部長通知:大量調理施設衛生管理マニュアル,食安発第 0829008 号(2003)
23) Rook J. J.: Environ. Sci. Technol, 11(5), p478-482 (1977)
24) 富田基郎他: 衛生化学, 28, p21-27 (1982)
25) 杉野邦雄他: 水質汚濁研究, 9(7), p437-444 (1986)
26) 日本食品洗浄剤衛生協会: 次亜塩素酸ナトリウム, p13-15 (2002)
27) Streicher, R. P. et al.: Analytical Letter, 19(5-6), p681-696 (1986)
28) 健康・栄養情報研究会：国民栄養の現状 平成14年厚生労働省国民栄養調査結果, p114 (2004)
29) De Angelo AB et al.: J. Toxicol. Environ. Health, 58, 485-507 (1999)
30) De Angelo AB et al. : J. Toxicol. Environ. Health, 52, p425-445 (1997)

H. 研究発表

1．論文発表　なし

2．学会発表　なし

I. 知的財産権の出願・登録状況

1．特許取得　なし

2．実用新案登録　なし

3．その他　なし

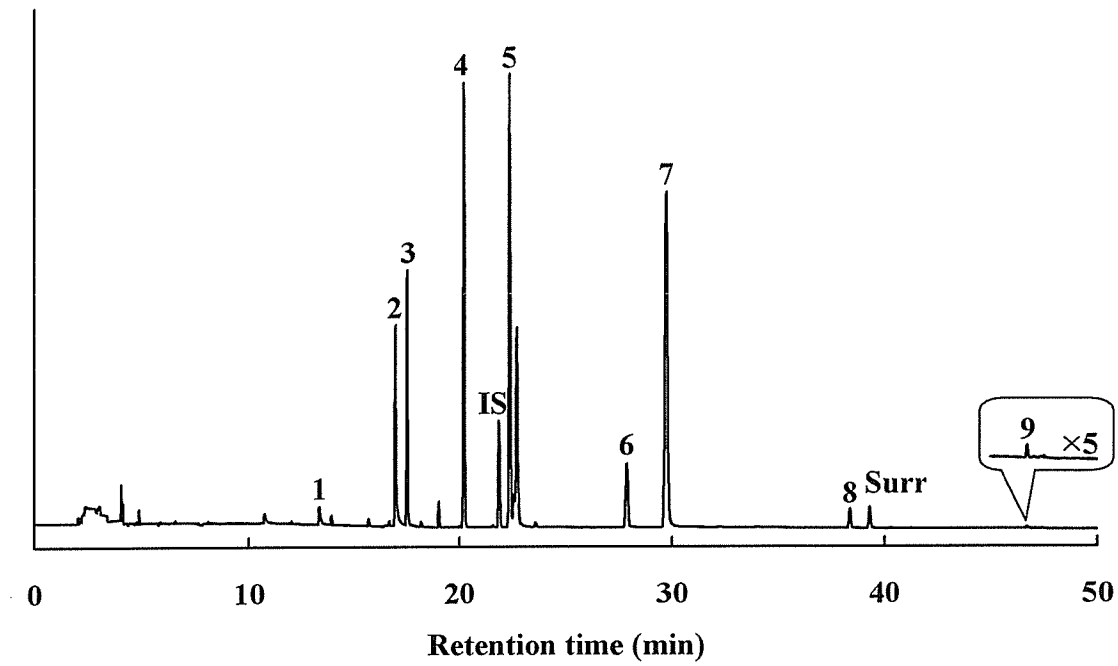

Fig.1. ハロ酢酸類混合標準液誘導体の GC/ECD クロマトグラム

1: Monochloroacetic acid (MCAA), 2: Monobromoacetic acid (MBAA), 3: Dichloroacetic acid (DCAA), 4: Trichloroacetic acid (TCAA), 5: Bromochloroacetic acid (BCAA), 6: Dibromoacetic acid (DBAA), 7: Bromodichloroacetic acid (BDCAA), 8: Chlorodibromoacetic acid (CDBAA), 9: Tribromoacetic acid (TBAA), IS: 1,2,3-Trichloropropane, Surr: 2,3-Dibromoacetic acid

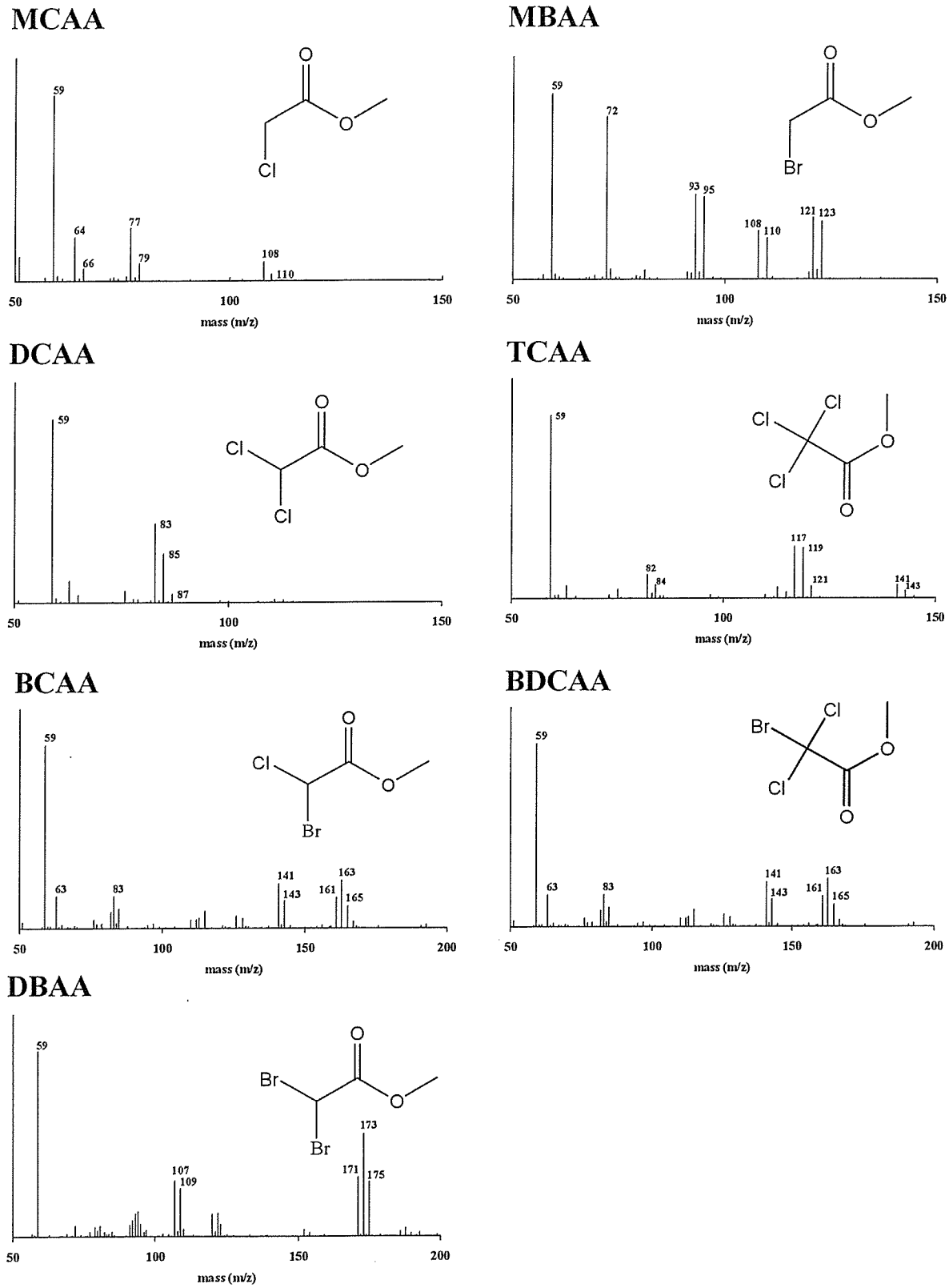

Fig.2. ハロ酢酸メチルエステルの GC/MS マススペクトル

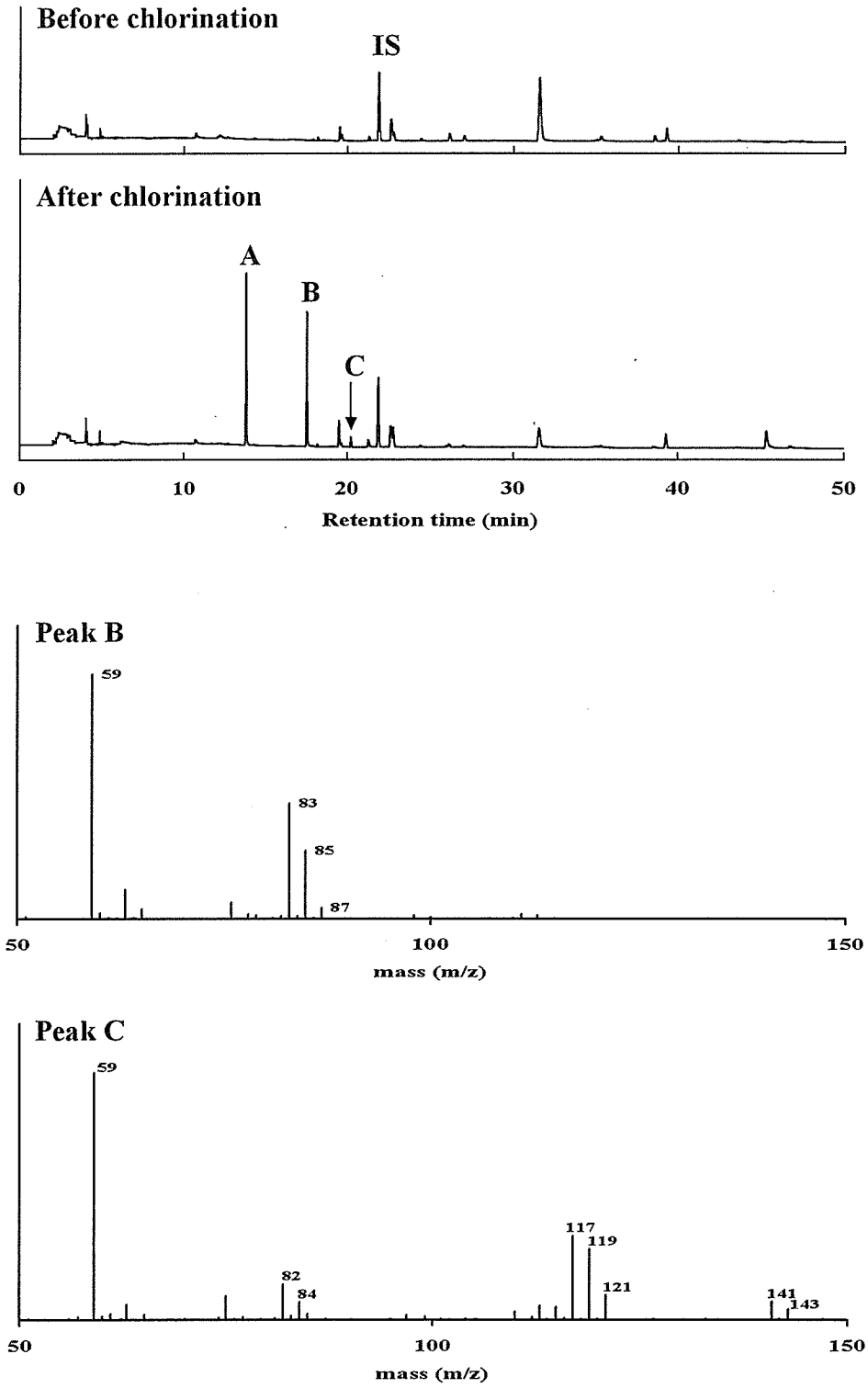

Fig.3. 次亜塩素酸ナトリウムにより殺菌処理したカット野菜試験液の GC/ECD クロマトグラム及びマススペクトル

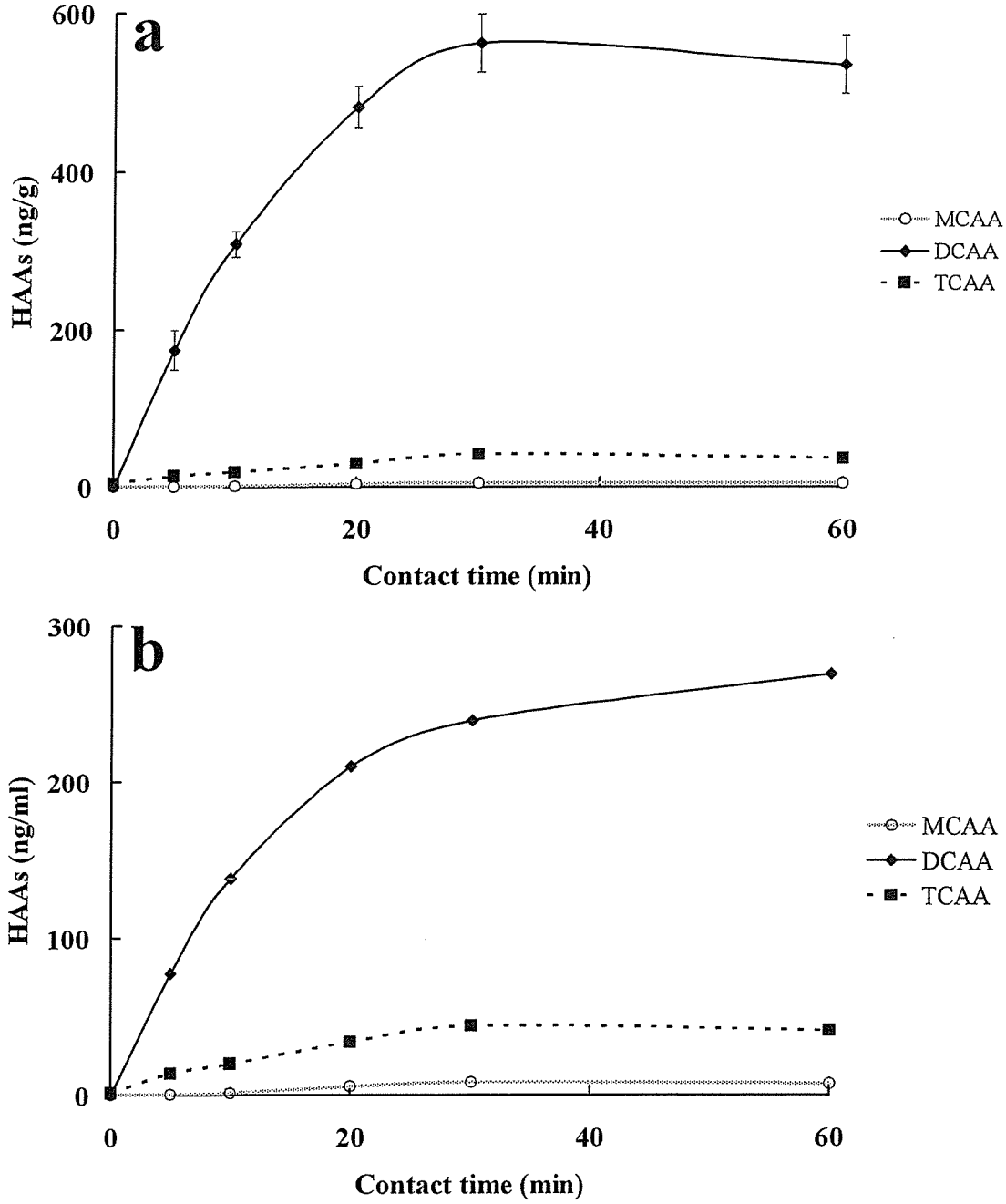

Fig.4. 次亜塩素酸ナトリウム処理カット野菜中におけるハロ酢酸生成量の経時変化. a)カット野菜中のハロ酢酸の推移, b)次亜塩素酸ナトリウム浸漬液中のハロ酢酸生成量の推移

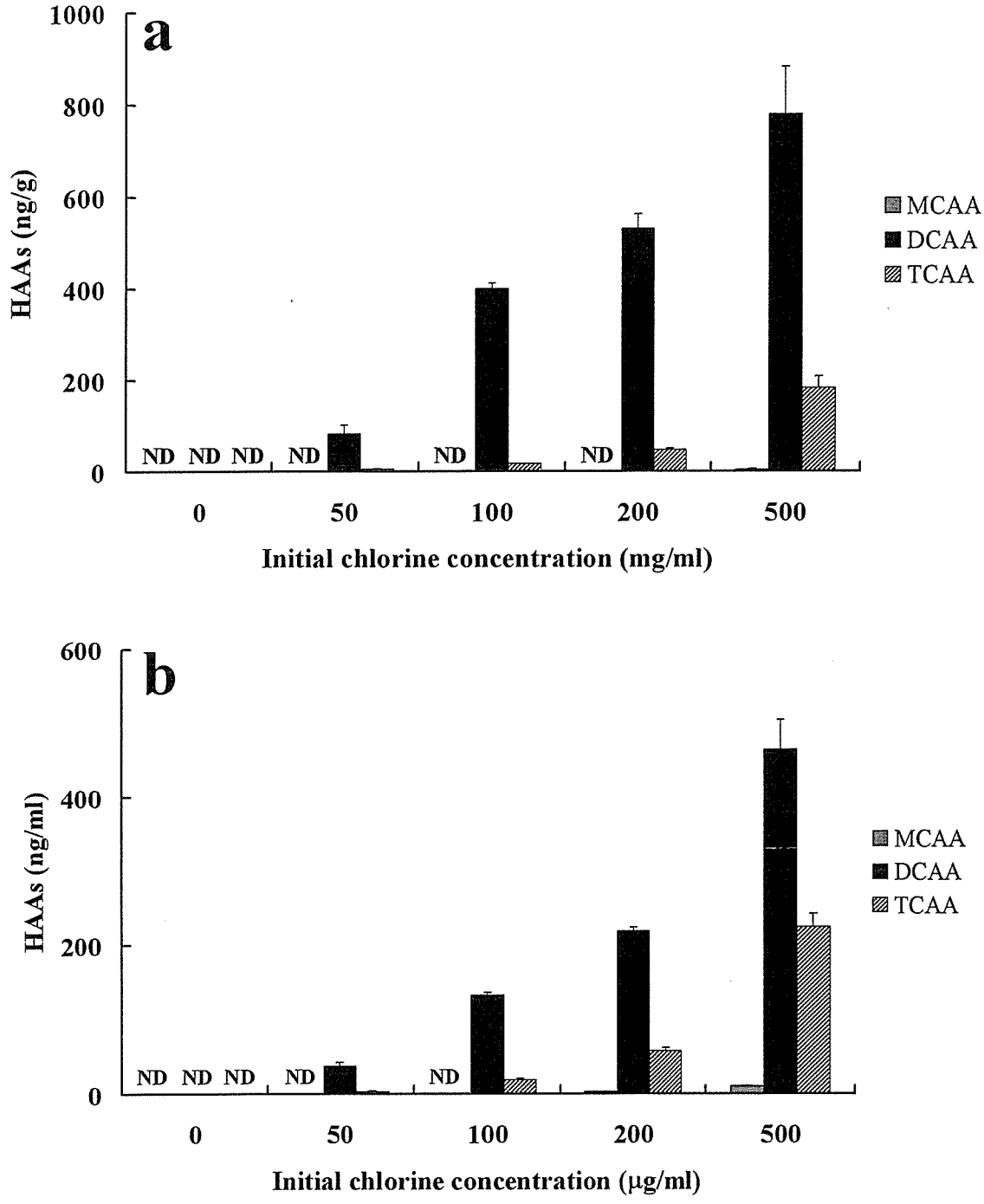

Fig.5. 次亜塩素酸ナトリウム濃度によるカット野菜中のハロ酢酸生成量の変化. a)カット野菜中のハロ酢酸の生成量, b)次亜塩素酸ナトリウム浸漬液中のハロ酢酸の生成量

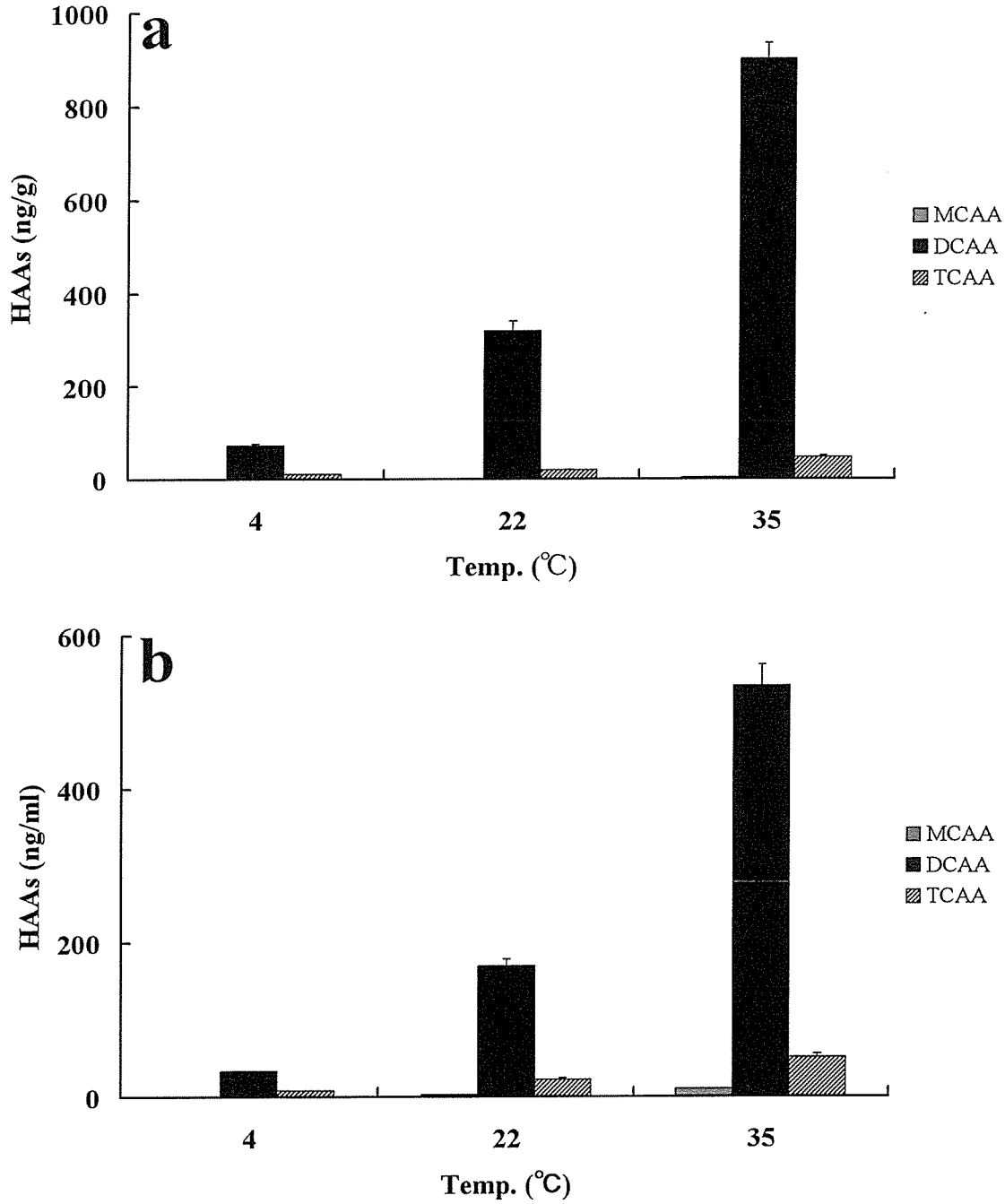

Fig.6. 次亜塩素酸ナトリウム浸漬液の温度によるカット野菜中のハロ酢酸の変化. a) カット野菜中のハロ酢酸の生成量, b) 次亜塩素酸ナトリウム浸漬液中のハロ酢酸の生成量

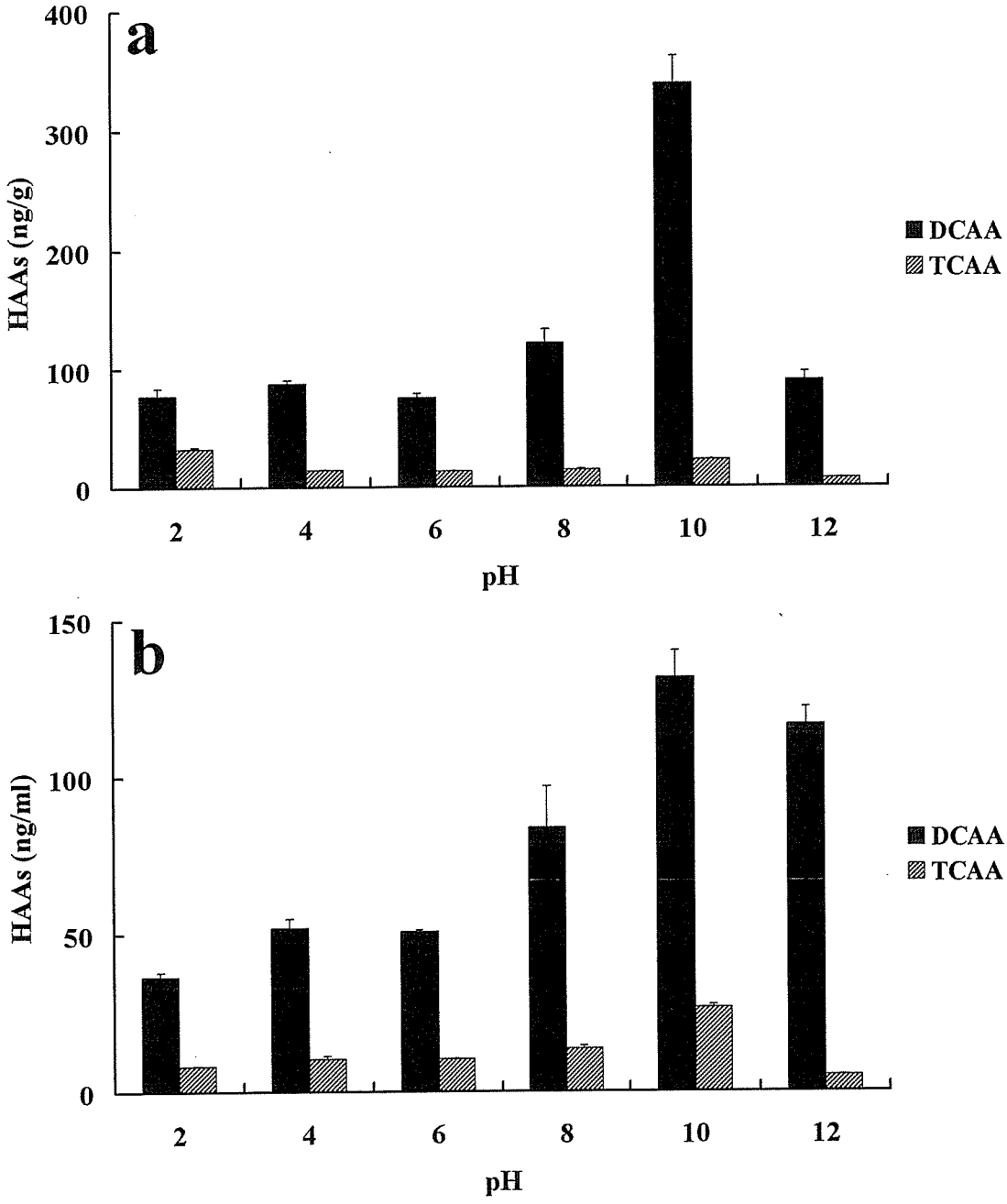

Fig.7. 次亜塩素酸ナトリウム浸漬液の pH によるカット野菜中のハロ酢酸生成量の変化. a)カット野菜中のハロ酢酸の生成量, b)次亜塩素酸ナトリウム浸漬液中のハロ酢酸の生成量

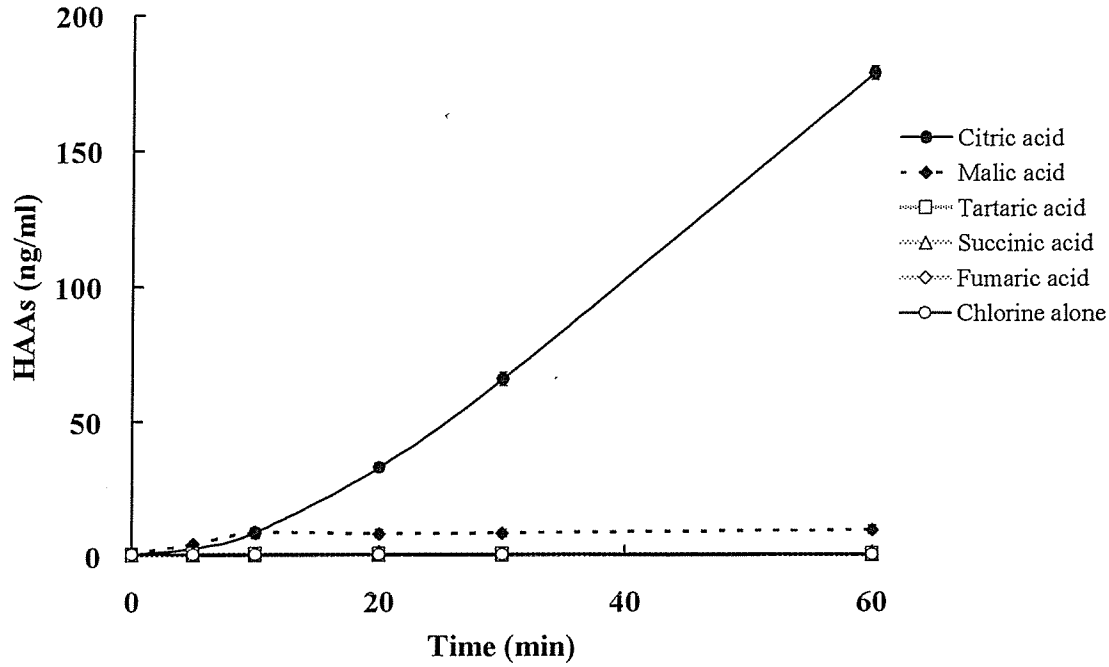

Fig.8. 次亜塩素酸ナトリウム・有機酸混合溶液における有機酸混和後のジクロロ酢酸生成量の推移.

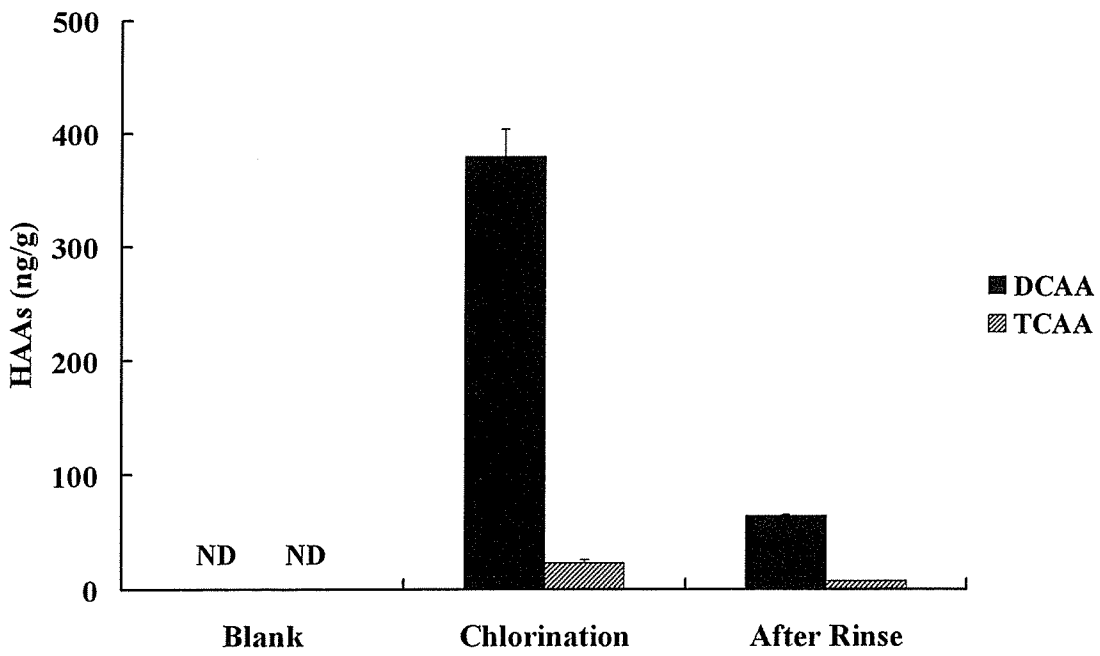

Fig.9. 次亜塩素酸ナトリウム処理により生成したハロ酢酸の水洗浄による除去効果

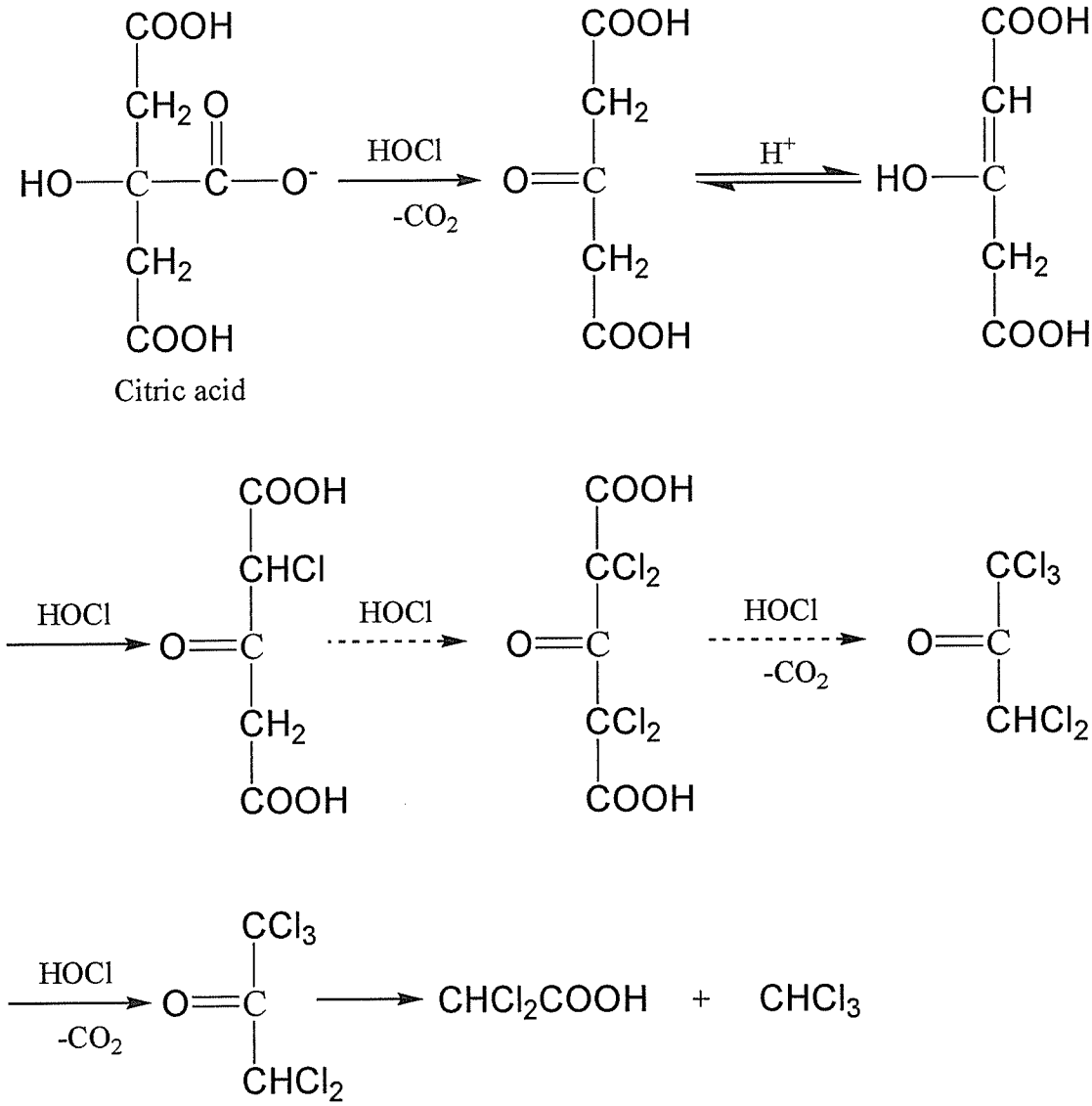

Fig.10. クエン酸の次亜塩素酸ナトリウムによるクロロホルム及びジクロロ酢酸生成メカニズム(仮説)

Table 1. GC/ECD によるハロ酢酸のカット野菜からの添加回収試験

No.	Compounds	Amount of added HAAs			
		50 ng/g		500 ng/g	
		平均(%)	標準偏差	平均(%)	標準偏差
1.	Monochloroacetic acid	86.6	6.7	91.3	2.1
2.	Monobromoacetic acid	98.4	5.0	94.4	1.9
3.	Dichloroacetic acid	102.7	2.1	99.3	1.2
4.	Trichloroacetic acid	102.3	1.8	100.9	0.9
5.	Bromochloroacetic acid	103.1	1.6	101.3	1.3
6.	Bromodichloroacetic acid	92.0	7.0	94.8	2.0
7.	Dibromoacetic acid	105.0	1.6	102.8	1.4
8.	Chlorodibromoacetic acid	-	-	91.4	2.4
9.	Tribromoacetic acid	-	-	-	-

* n=5

Table 2. GC/MS によるハロ酢酸のカット野菜からの添加回収試験

No.	Compounds	Amount of added HAAs			
		50 ng/g		500 ng/g	
		平均(%)	標準偏差	平均(%)	標準偏差
1.	Monochloroacetic acid	82.4	2.5	85.3	2.1
2.	Monobromoacetic acid	89.1	6.6	83.0	1.1
3.	Dichloroacetic acid	86.8	2.1	84.1	3.0
4.	Trichloroacetic acid	84.8	4.2	89.4	4.0
5.	Bromochloroacetic acid	87.4	2.4	91.1	0.9
6.	Bromodichloroacetic acid	87.3	3.6	80.5	2.8
7.	Dibromoacetic acid	89.9	4.4	90.9	4.0
8.	Chlorodibromoacetic acid	-	-	90.7	3.8
9.	Tribromoacetic acid	-	-	89.6	10.5

* n=5

研究成果の刊行に関する一覧表

雑誌

発表者氏名	論文タイトル名	発表誌名	巻号	ページ	出版年
Sugimoto, N., Yomota, C., Furusho, N., Sato, K., Yamazaki, T., Tanamoto, K.,	Application of liquid chromatography-nuclear magnetic resonance *spectroscopy* to the identification of ethyldimethylpyrazine, a food flavoring agent	Food Add. Contam.	23(12)	1253-1259	2006
Kitamura, Y., Iwasaki T., Saito, M., Mifune, M., Saito, Y., Sato, K., Yomota C., Tanamoto K	Standard Infrared Absorption Spectrum of Betaine and Optimal Conditions for its Measurement	J. Food Hygienics Society of Japan	47(5)	232-236	2006
Sugimoto, N., Koike, R., Furusho, N., Tanno, M., Yomota, C., Sato, K., Yamazaki, T., Tanamoto, K.,	Quantitative nuclear magnetic resonance spectroscopy determination of the oxyethylene group contents of polysorbates	Food Add. Contam.	accepted		2007
Mine, T., Okada, Y. and Semma, M	The interaction of sorbic acid with amino acid may alter the quality of foods somewhere in the food chain from production to table	Jpn. J.Food Chem.	In press		2007

Food Additives and Contaminants, December 2006; 23(12): 1253–1259

Taylor & Francis
Taylor & Francis Group

Application of liquid chromatography–nuclear magnetic resonance spectroscopy for the identification of ethyldimethylpyrazine, a food flavouring agent

NAOKI SUGIMOTO, CHIKAKO YOMOTA, NORIKO FURUSHO, KYOKO SATO, TAKESHI YAMAZAKI, & KENICHI TANAMOTO

National Institute of Health Sciences, 1-18-1 Kamiyoga, Setagaya, Tokyo 158-8501, Japan

(Received 24 April 2006; revised 20 June 2006; accepted 20 June 2006)

Abstract
The application of liquid chromatography–nuclear magnetic resonance spectroscopy (LC–NMR) for the direct identification of ethyldimethylpyrazine, a food flavouring agent, has been studied. The commercial product is a mixture of two regio-isomers, 2-ethyl-3,5-dimethylpyrazine (1) and 2-ethyl-3,6-dimethylpyrazine (2); however, the exact composition of the mixture is unknown. Structural characterization by LC–MS and GC–MS was not possible because both regio-isomers yield the same molecular related ion and ion fragmentation. To rapidly identify the two regio-isomers, the product was analyzed by LC–NMR with on-flow and fraction loop modes. From the results, the structure elucidations of the two regio-isomers could be carried out without the need to isolate the isomers by the usual procedures.

Keywords: *Food additive, dimethylethylpyrazine, flavouring agent, LC–MS, GC–MS, LC–NMR*

Introduction

Recently, gas chromatography–mass spectrometry (GC–MS) and liquid chromatography–mass spectrometry (LC–MS) have been widely exploited, with a massive growth of applications, particularly in food safety, and especially in the identification and quantification of bioactive constituents, food additives and contaminants. Despite these advances, MS by itself does not always provide definitive structural identification, and nuclear magnetic resonance (NMR) spectroscopic data are often required. NMR has played an important role in analytical chemistry but conventional NMR spectroscopic analysis has required time-consuming isolation and purification steps. Recently, on-line liquid chromatography–nuclear magnetic resonance (LC–NMR) has been developed and can provide structural information that complements LC–MS and GC–MS data, facilitating rapid analyses of mixtures without the need for isolation. The applications of LC–NMR to drug metabolism, natural products identification and characterization of isomeric mixtures have been reviewed (Wolfender et al. 1998, 2001; Iwasa et al. 2003; Sohda et al. 2004; Waridel et al. 2004).

Ethyldimethylpyrazine is a flavouring agent permitted for use in foods since December 2004 in Japan. The substance is used widely for adding the flavour of roasted nuts to chocolate, cookies, etc. (Goldman et al. 1967; Ohta et al. 1987; Buchi and Galindo 1991; Burdock 1997). The commercial flavouring agent product consists of two regio-isomers, 2-ethyl-3,5-dimethylpyrazine (1) and 2-ethyl-3,6-dimethylpyrazine (2), as shown in Figure 1. FAO/WHO Joint Expert Committee on Food Additives (JECFA) had evaluated a mixture of two isomers of ethyldimethylpyrazine. JECFA concluded this flavouring agent was of "no safety concern" based on current intake, but safety evaluation of each isomer was not carried out (WHO Food Additives Series 48). The relative amounts of 1 and 2 in the commercial product are not specified, and the composition of the mixture is

Correspondence: N. Sugimoto. E-mail: nsugimot@nihs.go.jp

ISSN 0265-203X print/ISSN 1464-5122 online
DOI: 10.1080/02652030600871168

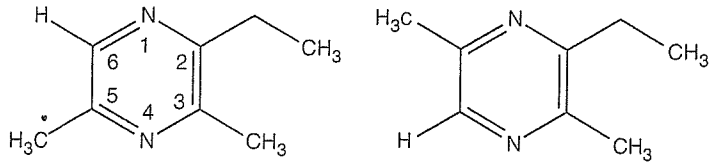

2-ethyl-3,5-dimethylpyrazine (1) 2-ethyl-3,6-dimethylpyrazine (2)

Figure 1. Structures of 2-ethyl-3,5-dimethylpyrazine (1) and 2-ethyl-3,6-dimethylpyrazine (2).

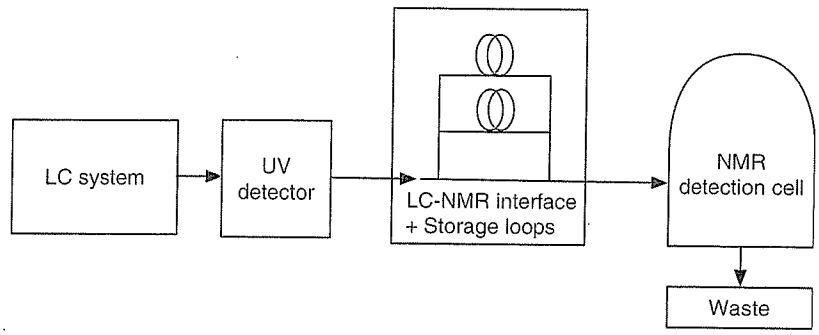

Figure 2. Schematic of LC–NMR system. The LC system is connected to the NMR detection cell through a UV detector. On on-flow mode, real-time sequence of ^{1}H-NMR is acquired after the constituents are separated by the LC system. On fraction loop mode, the separated constituents are collected into fraction storages with trigger of UV detection and then each constituent is moved to NMR detection cell.

not easily determined because standards for the two regio-isomers are not commercially available. Therefore, to establish the quality control of this flavouring agent, it is important to develop a detection method without standards. In this paper, we report the application of LC–NMR to the direct identification of the two regio-isomers of ethyldimethylpyrazine as part of studies to evaluate its quality and safety as a food flavouring agent in Japan.

Materials and methods

Materials

A sample of commercial ethyldimethylpyrazine product was obtained through the Japan Food Additives Association. Acetonitrile (CH_3CN) was of HPLC grade and was used without further purification. NMR solvents, deuterium oxide (D_2O) and acetonitorile-d_3 (CD_3CN) were purchased from Isotec Inc. (Miamisburg, OH, USA).

Instrumentation

The LC–MS system (Waters, Milford, MA, USA) consisted of an Alliance 2695 HPLC, a 2996 photodiode array detector (PDA) and a ZQ single-quadropole mass spectrometer (MS) equipped with a Z-spray electrospray interface. The GC–MS system (Shimadzu, Kyoto, Japan) consisted of a GC-17A GC and QP-5050A MS. The LC–NMR system consisted of a NANOSPACE SI-2 series HPLC (Shiseido, Tokyo, Japan) equipped with storage loops for fraction mode and a JNM-ECA (500 MHz; JEOL, Tokyo, Japan) installed HX/FG LC probe (JEOL). The diagrammatic illustration of LC–NMR system is shown in Figure 2.

LC–MS and GC–MS analyses

Commercial ethyldimethylpyrazine product (10 µl, liquid) was dissolved in CH_3CN (1.0 ml) and 1 µl of the solution was then injected into the LC–MS and GC–MS systems under the following conditions. LC–MS conditions: column: TSK-gel ODS-80TsQA (2.0 mm I.D. × 250 mm) (Tosoh, Tokyo, Japan); mobile phase: water/CH_3CN (20:80, v/v); flow-rate: 0.1 ml min^{-1}; The on-line PDA detector was monitored between 192 and 400 nm, and peak detections were at UV 278 nm. The electrospray source ran at 3.0 kV capillary voltage, 120 and 350°C source and desolvation temperatures, respectively, and 350 and 50 l h^{-1} desolvation and cone gas flow-rates, respectively. The cone voltage was 30 V for positive-ion detection. Full-scan acquisition between *m/z* 50 and 300 was performed at a scan speed of 0.1 s scan^{-1} with a 0.1-s inter-scan delay.

GC–MS conditions: column: Inert Cap WAX (0.25 mm I.D. × 30 m, 0.25 μm thickness (GL Sciences, Tokyo, Japan)); column temperature: 50°C → 5°C min^{-1} → 230°C (4 min); inject temperature: 250°C; carrier gas: He, 1.5 ml min^{-1}; split ratio: 1:200; ionization voltage: 70 eV; accelerator voltage: 1.0 kV; scan range: *m/z* 50–300. Mass spectra were referred to the NIST 147 database.

LC–NMR and NMR analyses

Commercial ethyldimethylpyrazine product (20 μl) was dissolved in D_2O/CH_3CN (20:80, v/v) (1.0 ml) and 2 μl of the solution was injected into the LC–NMR system. LC–NMR was performed under the following conditions: column: TSK-gel ODS-80TsQA (2.0 mm I.D. × 250 mm) (Tosoh); mobile phase: D_2O/CH_3CN (20:80, v/v); flow-rate: 0.1 ml min^{-1}; detection, UV 278 nm. LC–NMR spectra were recorded in the two-dimensional (2D) on-flow and fraction loop modes using a HX/FG LC probe with a flow cell of 60 μl active volume at 30°C. Water suppression enhanced through T1 effect (WET) solvent suppression (Smallcombe et al. 1995) and related sequences were used to suppress the peaks of CH_3CN, its ^{13}C satellites and the residual HOD in D_2O. In the 2D on-flow mode, FID was collected with 4K data points, and eight scans with 1 s repletion time were accumulated; other parameters were the defaults for conventional NMR depending on JEOL. In fraction loop mode, FIDs of the two regio-isomers were collected with the conventional default parameters and over 200 scans were accumulated, respectively. Assignments of proton and carbon signals were confirmed by pulse-field gradient (PFG) heteronuclear multiple quantum coherence (HMQC) and PFG heteronuclear multiple bond connectivity (HMBC) experiments with WET (Smallcombe et al. 1995).

Results and discussion

LC–MS and GC–MS analyses of commercial ethyldimethylpyrazine product

To estimate the relative amounts of the two regio-isomers, 2-ethyl-3,5-dimethylpyrazine (**1**) and 2-ethyl-3,6-dimethylpyrazine (**2**), in the commercial product, LC–MS and GC–MS were performed. The LC profile of the commercial product with detection at 278 nm is shown in Figure 3. The separation of two regio-isomers was accomplished using isocratic LC separation, and two peaks were observed at 31.9 and 33.8 min at 278 nm, which must be derived from **1** or **2**, respectively. The PDA spectra of peaks A and B, and the ESI–MS (positive mode) with the molecular-related ion peak at *m/z* 137 $[M+H]^+$ were almost identical (Figure 4). Furthermore, although in-source collision-induced decomposition (CID) experiments were performed by varying the sampling-cone voltage ($\Delta V = 30$ V), peaks A and B showed that the same fragment ions at *m/z* 59, 83, 102 and 116 with very similar intensities. Thus, the difference between peaks A and B was not observed by PDA and ESI–MS spectra.

The GC–MS profile is shown in Figure 3. Two peaks X and Y were observed at 10.6 and 11.0 min from the total ion chromatogram. The area magnitudes of peaks X and Y were 43.4 and 56.6, respectively, and was very close to the area ratio of peaks B and A (B/A = 45.0:55.0), which was observed at 278 nm on LC. Therefore, we presumed that peaks X and Y on GC correspond to peak B and A on LC, respectively. The EI–MS spectra of peaks X and Y are shown in Figure 5. The EI–MS spectra of peaks X and Y had no significant differences, and the relative intensities of fragment ions at *m/z* 56, 107 of peak Y differed only slightly from the corresponding fragment ions for peak X. Although the spectra of peaks X and Y were referred to the NIST 147 database, unambiguous identification could not be provided. Therefore, it was concluded that the structural determinations of the two regio-isomers in the commercial ethyldimethylpyrazine product by LC–MS and GC–MS was impossible.

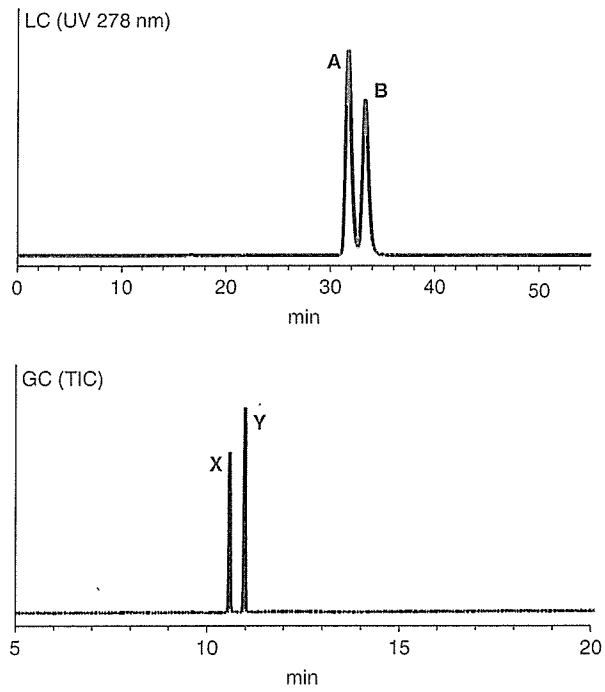

Figure 3. LC and GC profiles of commercial ethyldimethylpyrazine product. GC and LC conditions are described in the experimental section.

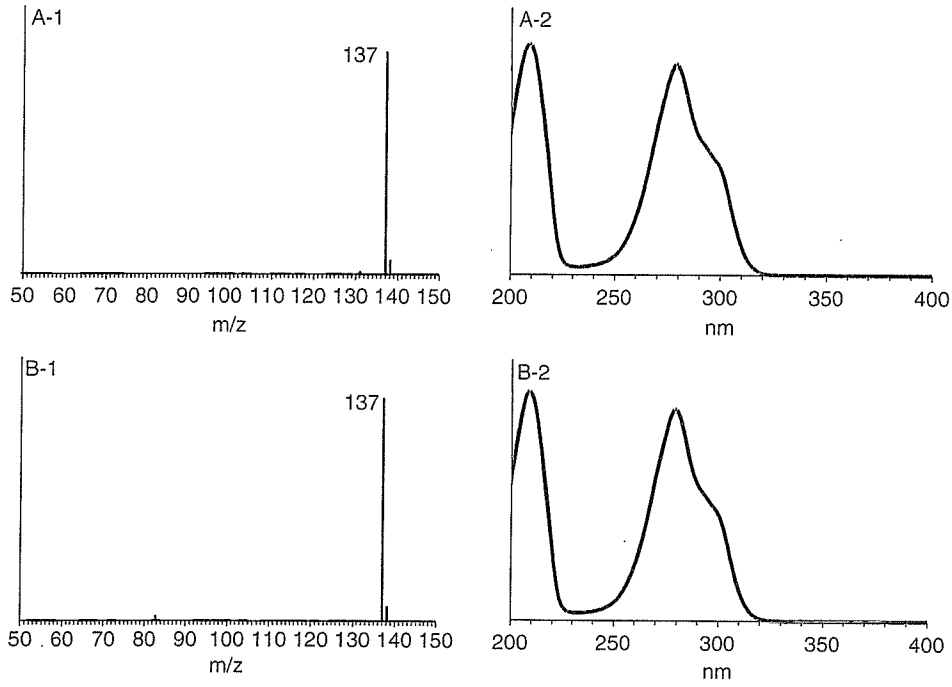

Figure 4. ESI–MS and PDA spectra of peaks A and B. (A-1) ESI–MS of peak A. (A-2) PDA of peak A. (B-1) ESI–MS of peak B. (B-2) PDA of peak B.

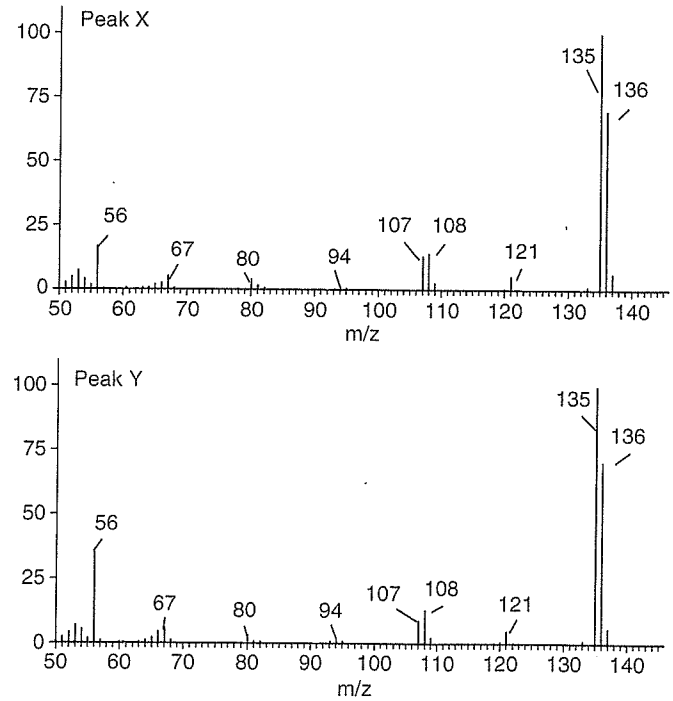

Figure 5. EI–MS spectra of peaks X and Y.

Determination of regio-isomers of ethyldimethylpyrazine by LC–NMR

As a preliminary step, we obtained the ^{1}H-NMR spectrum of the commercial product of ethyldimethylpyrazine using conventional NMR spectroscopy without separation, but it was difficult to distinguish signals of two regio-isomers because most signals overlapped except δ 8.36 and 8.38 ppm signals on the pyrazine ring of each regio-isomer. Also, the coupling constants (J) of most of signals could not be read exactly. Thus, it was necessary for

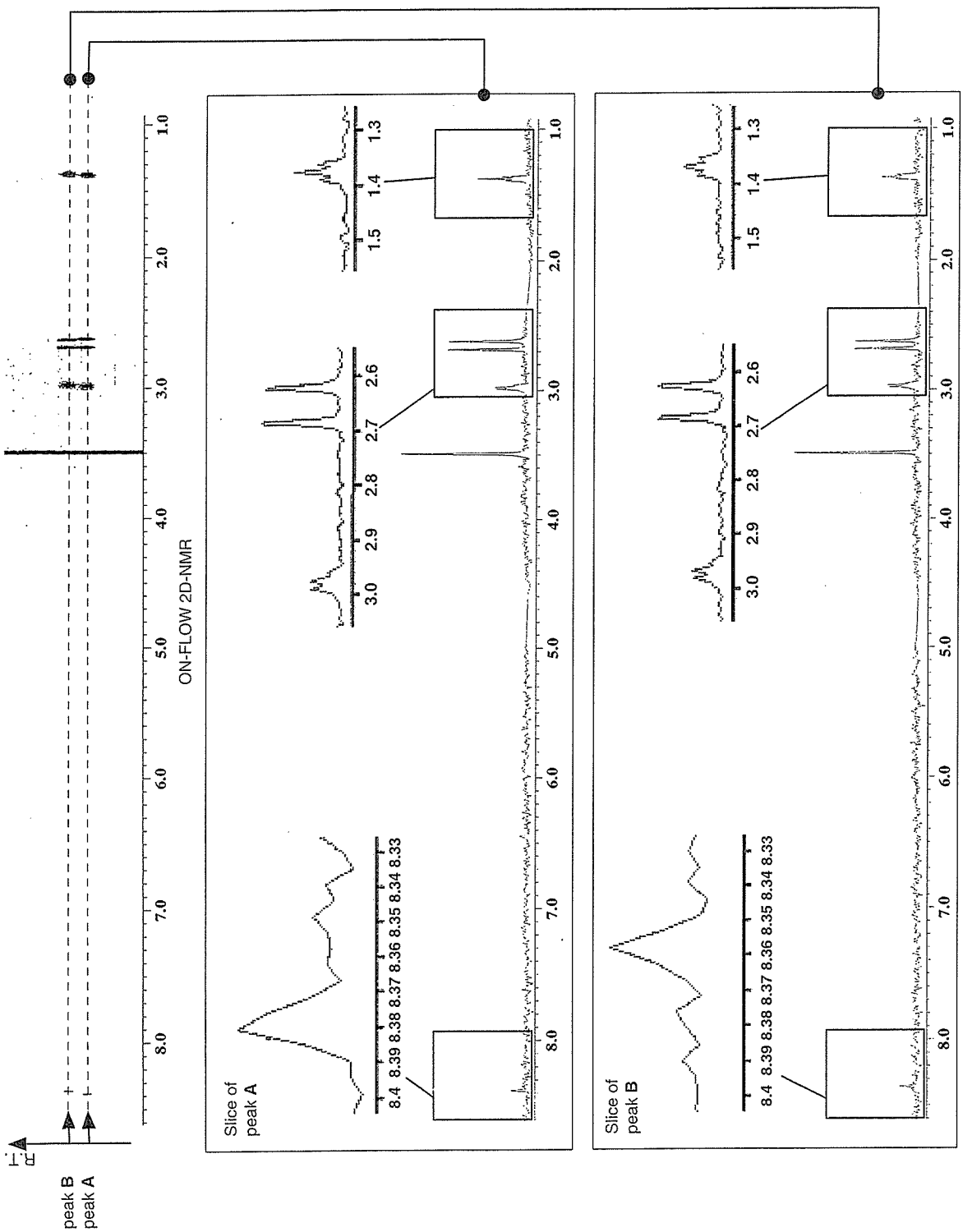

Figure 6. ^{1}H-NMR data of peaks A and B using 2D on-flow mode LC–NMR.

Table I. NMR data (δ, ppm, D_2O/CH_3CN (20:80, v/v)) for peaks A (1) and B (2).

	Peak A			Peak B		
	2-Ethyl-3,5-dimethylpyrazine (1)			2-Ethyl-3,6-dimethylpyrazine (2)		
No.	^1H	^{13}C	HMBC	^1H	^{13}C	HMBC
2	–	161.7	–	–	162.0	–
3	–	155.0	–	–	155.0	–
5	–	155.0	–	8.36 (1H, s)	141.9	C-3, C-6
6	8.38 (1H, s)	141.3	C-2	–	154.5	–
3-CH_3-	2.68 (3H, s)	20.9	C-2, C-3	2.69 (3H, s)	20.9	C-2, C-3
6-CH_3-	–	–	–	2.63 (3h, s)	20.9	C-5, C-6
5-CH_3-	2.62 (3H, s)	20.7	C-5, C-6	–	–	–
2-CH_3-CH_2-	1.38 (3H, t, J=7.5 Hz)	12.7	C-2	1.37 (3H, t, J=7.5 Hz)	13.1	C-2
2-CH_3-CH_2-	2.98 (2H, q, J=7.5 Hz)	27.8	C-2	2.97 (2H, q, J=7.5 Hz)	27.9	C-2

^{13}C chemical shifts were assigned indirectly by HMQC and HMBC.

identification and structural determination of two regio-isomers to carry out a separation. However, general preparative separations, which consist of isolation and purification steps, are time-consuming and tedious. We concluded that LC–NMR would be an ideal method for obtaining NMR spectral information for individual isomers.

The mixture of two regio-isomers was first analyzed by on-flow mode LC–NMR using LC conditions identical to LC–MS. By on-flow mode, NMR spectra of a mixture of two regio-isomers of ethyldimethylpyrazine were displayed as a 2D matrix showing NMR spectrum against retention time, similar to an LC–PDA plot. Figure 6 shows the 2D data for the NMR region from δ 1 to 9 ppm. So the individual spectra of regio-isomers could be extracted from 1D slices along the x-axis, the stacked plots were sliced from each retention time of peaks A and B, and the coupling constants and chemical shifts could be read. However, it was not possible to determine each isomer structure from 1D slice data because the resolution in the individual spectra was lower than that of conventional NMR and the signals were very similar, except the δ 8.36 and 8.38 ppm signals on the pyrazine ring of each regio-isomer. On on-flow mode, it is impossible to carry out 2D-NMR data, such as HMQC and HMBC, which provide more structural information, because these 2D-NMR experiments need more accumulation time than ^1H-NMR.

To determine the individual isomers exactly, the mixture was analyzed by fraction loop mode LC–NMR (Figure 2). Using fraction loop mode, the fractions of the eluent flowing from LC system were separated by a storage device that consisted of fraction loops. Without interrupting the separation, peaks could be trapped in the fraction loops. The fractionated peaks were transferred into a LC–NMR probe, respectively, and NMR spectra of each peak could be carried out as with conventional NMR. The resolution is also better than that of on-flow mode.

After peaks A and B were fractionated into the loops using the same conditions for LC–MS, the contents in the loops were transferred into a LC–NMR probe. Accumulated times of 200 were used to get unambiguous spectral data of ^1H-NMR and 2D HMQC and HMBC. The results were two sets of spectra for peaks A and B (Table I). ^{13}C-NMR data could not be observed directly on LC–NMR because the amount of samples was insufficient. This was a disadvantage against conventional NMR but the ^{13}C-NMR data could be indirectly attributed from correlations of 2D HMQC and HMBC experiments. The observed HMBC correlations are listed in Table I. The ^1H-NMR spectrum of the content of peak A exhibited five proton signals at δ 8.38 (1H, s), 2.68 (3H, s), 2.62 (3H, s), 1.38 (3H, t, J=7.5 Hz) and 2.98 (2H, q, J=7.5 Hz), which were attributed to a proton on the pyrazine ring, two methyl protons, and methyl and ethylene protons on the ethyl group, respectively. ^{13}C-NMR data was also attributed indirectly by HMQC. A HMBC correlation was observed between methyl protons on the ethyl group at δ 1.38 and quaternary carbon signal at δ 161.7, suggesting the carbon signal was at C-2. Furthermore, a proton on the pyrazine ring at δ 8.38 was correlated to C-2 carbon. Based on these result, the structure of the content of peak A was determined as 2-ethyl-3,5-dimethylpyrazine (1). On the other hand, as no correlation was observed between a proton on the pyrazine ring at δ 8.36 (H-5) and quaternary carbon signal at δ 162.0, the structure of the content of peaks B was determined as 2-ethyl-3,6-dimethylpyrazine (2). It took only 2 days to determine the structures of two regio-isomers using LC–NMR, but it would take over 1 week using general isolation and purification.